Printed in the Republic of Korea
ANALYTICAL SCIENCE & TECHNOLOGY
Vol. 34 No. 2, 87-98, 2021
https://doi.org/10.5806/AST.2021.34.2.87

Development of a nanoparticle multi-generator for assessment of inhalation hazard

Sung-Bae Lee[1,★], Jeong-Hee Han[1], Tae-Hyun Kim[1], Hyo-Geun Cha[1], and Cheal-Hong Lim[1]

[1]*Inhalation Toxicology Research Center, Occupational Safety & Health Research Institute, 30 Expo-ro 339beon-gil Yuseong-gu Daejeon, 34122, Republic of Korea*

(Received November 17, 2020; Revised January 28, 2021; Accepted February 4, 2021)

Abstract: In this study, we developed the nanoparticle multi-generator by 3D printer fusion deposition modeling (FDM) method that can reliably generate and deliver nanoparticles at a constant concentration for inhalation risk assessment. A white ABS filament was used as the test material, and SMPS was used for concentration analysis such as particle size and particle distribution. In the case of particle size, the particle size was divided by 100 nm or less and 100 to 1,000 nm, and the number of particles concentration, mass concentration, median diameter of particles, geometric average particle diameter, etc were measured. The occurrence conditions were the extruder temperature, the extruding speed of the nozzle, and the air flow rate, and experiments were conducted according to the change of conditions including the manufacturer's standard conditions. In addition, the utility of inhalation risk assessment was reviewed through a stability maintenance experiment for 6 h. As a result of the experiment, the size of the nanoparticles increased as the discharger temperature increased, as the discharge speed of the nozzle increased, and as the air flow rate decreased. Also, a constant pattern was shown according to the conditions. Even when particles were generated for a long time (6 h), the concentration was kept constant without significant deviation. The distribution of the particles was approximately 80 % for particles of 60 nm to 260 nm, 1.7 % for 1 μm or larger, 0.908 mg/m^3 for the mass concentration, 111 nm for MMAD and 2.10 for GSD. Most of the ABS particles were circular with a size of less than 10 nm, and these circular particles were aggregated to form a cluster of grape with a size of several tens to several hundred nm.

Key words: nanoparticle, 3D printer, multi-generator, inhalation toxicity

1. Introduction

Several fields commonly use polymeric substances in extruders and injection molders. Recently, the use of three-dimensional (3D) printers and pens to create industrial prototypes, figures, and other structures at homes and offices outside business facilities has increased. In fact, in the process of molding via a 3D printer, the polymeric material is inhaled into the human body. The fume, a solid-phase steam of

★ Corresponding author
Phone : +82-(0)42-869-8513 Fax : +82-(0)42-869-8693
E-mail : sblee@kosha.or.kr

nanoparticles generated upon the use of 3D printers, can be toxic to the human body as it enters the respiratory system. 3D printers are used in the fabrication of 3D molds by depositing liquid or powder materials such as polymers or metals. The use of 3D printers enables a substantial reduction in costs and time as well as enables personalized fabrication, as even complicated 3D molds can be easily created. These advantages have led to the use of 3D printers in various industries, such as motor vehicles, aircraft, construction, health care, home appliances, and toys.

Nanoparticles, also known as ultrafine particles, are defined as particles of size ≤100 nm. For fibrous materials, the particles should be <100 nm in both directions. The inhalation of such ultrafine particles into the human respiratory system can cause various health hazards and respiratory diseases as they can pass through the alveoli. Studies on the hazardous from unintentionally generated nanoparticles in 3D printers have evoked the need for identification of each substance generated. However, the specific impact of the inhalation of such substances by a worker at different concentrations has not been clearly identified yet,[1-5] owing to insufficient evidence from studies on the monitoring and assessment of the potential health risks of nanoparticles and HAPs generated in 3D printing. A recent study by Floyd et al.[6] claimed the need for toxicity analysis of the fume generated by 3D printers, and Park *et al*.[5] suggested that studies should be continuously conducted regarding 3D printing with respect to environmental health sciences.

At present, there is an urgent need to establish a scientific basis for the criteria to determine the health risks of nanoparticles according to the processing method of polymeric materials. The nanoparticles generated in the 3D printing process are chemically stable and inert, being bio-persistent.[7] To conduct an assessment of inhalation hazards, nanoparticles with such bio-persistency should be generated at a constant, stable level in adequate concentrations. However, setting up many 3D printers in a given space to mediate the exposure to laboratory animals is inefficient and inappropriate, as the particle size and concentration would vary according to the printer location, distance, and operation conditions. Moreover, it is impossible to maintain constant concentrations in such a space as 3D printing leads to a cumulative increase in particle concentration. Thus, this study developed a nanoparticle multi-generator (NMG) to resolve one of the biggest challenges indicated by previous studies in conducting the assessment of nanoparticle biotoxicity.

2. Experimental Procedures

2.1. Printing model and materials

2.1.1. Printing model selection

The fused deposition modeling (FDM) was adopted as it is the most frequently used model in the 3D printing industry with low cost and ease of use. Depending on the materials, the model allows the fabrication of durable materials.

2.1.2. Materials

White acrylonitrile butadiene styrene (ABS) filament was used. Because ABS allows easy processing with outstanding durability, it is the most frequently used metal substituent in industrial fields producing components in electronic devices, helmets, and motor vehicles.

2.2. Nanoparticle multi-generator

The NMG (640 × 220 × 390, size: W × D × H, unit: mm) was produced as a closed-type (*Fig.* 1). The device has six generation parts inside the generation chamber, and through the control part connected to the device, the extruder temperature, nozzle extruding speed, air flow, and other conditions can be controlled.

2.3. Measurements

2.3.1. Scanning mobility particle sizer

The scanning mobility particle sizer (SMPS; Model: 5.416, Grimm Aerosol Tecknik, Germany) connected with a long differential mobility analyzer was used for particle monitoring. The size of the generated particles was classified within the range of 5 nm – 1 μm and after particle condensation using a

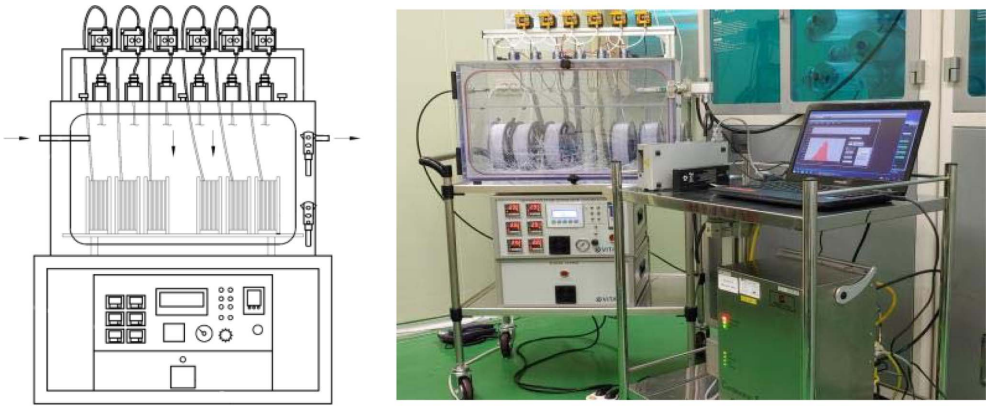

Fig. 1. The nano particle multi-generation system.

condensation particle counter, and the particle number and mass concentrations were measured using an optical detector. The aerosol diameter distribution was measured in real time in 4 min or 7 min intervals from the time before generation to the time at completion. The particle charge was neutralized using a neutralizer connected with an Am-241.

2.3.2. Electrical low-pressure impactor

The electrical low pressure impactor (ELPI; Dekati, Finland) allows the particles in the air to be charged and measured at a constant size in different intervals and was used as the corona charger. The air flow rate was 10 L/min, and the collection time was 65 min in the interval where the generation was maintained stable. The particles in the air were collected according to particle size (6 nm – 10 μm) in a cascade impactor comprising 14 steps. For the filter, greased aluminum foil (CFG-225, Dekati, Finland) was used, and the weight of the foil filter before and after mounting was measured to obtain the mass values.

2.3.3. Transmission electron microscopy

The transmission electron microscope (TEM; Model: H-7100FA, Hitachi-Instruments, Japan) was used to analyze the particle morphology and size. Aerosols were generated with the LC200-NI grid (Lacey/ Carbon 200 mesh, Nickel) installed at the interior and exterior of the generation chamber, and the size

Table 1. Information of filament and generating conditions

Condition	Material	Extruding nozzle size (nm)	Extruder temperature (°C)	Extruding speed (level)	Air flow rate (LPM)
Extruder temperature (°C)	ABS (White color)	0.4	**210**	10	30
	ABS (White color)	0.4	**240**	10	30
	ABS (White color)	0.4	**270**	10	30
	ABS (White color)	0.4	**300**	10	30
Extruding speed (level)	ABS (White color)	0.4	240	**5**	30
	ABS (White color)	0.4	240	**10**	30
	ABS (White color)	0.4	240	**15**	30
	ABS (White color)	0.4	240	**20**	30
Air flow rate (LPM)	ABS (White color)	0.4	240	10	**20**
	ABS (White color)	0.4	240	10	**30**
	ABS (White color)	0.4	240	10	**40**
	ABS (White color)	0.4	240	10	**50**

and morphology of particles in the collected air was analyzed.

2.4. Methods

The filament materials for the generation were provided to the extruder connected with the generation chamber, and the extruder temperature, nozzle extruding speed, and air flow rate were set (*Table* 1). Any foreign substances in the NMG such as the existing particles inside the chamber were expelled using the clean dry air through the HEPA filter. The SMPS was simultaneously run to verify the elimination of the particles in the chamber, and to measure the concentration before operation was measured. When the elimination was close to completion, the power to the heating wire was switched on to raise the temperature of the extruder connected with the heating wire, and as the extruder reached the set temperature, the filament materials were extruded to generate the particles.

2.5. Generator conditions

For particle generation, the conditions recommended by 3D printer and ABS filament manufacturers were followed: nozzle diameter at 0.4 mm, extruder temperature at 240 ºC, extruding speed at level 10 (50 s/cycle), and the recommended air flow rate.

The extruder temperature was adjusted in 30 ºC intervals as 210 ºC, 240 ºC, 270 ºC, 300 ºC, and the nozzle extruding speed was adjusted using the extruder stepper from the minimum level of 5 to the levels 10, 15, and 20. The air flow rate was set via mass flow controller to 20 LPM, 30 LPM, 40 LPM, and 50 LPM. In addition, for the long-term stability test, the generation was conducted for at least 6 h under the conditions recommended by the 3D printer and filament manufacturers.

2.6. Data analysis

For the particle number and mass concentrations measured during the time of generation, the analysis program provided by the SMPS manufacturer (Grimm Nano Software V1-5-0 (2015-08-21) & Grimm Aerosol Tecknik, Germany) was used. The data of particle number concentration (particles/cm^3) and particle mass concentration (μg/m^3) were expressed as the geometric mean (GM) and geometric standard deviation (GSD). In addition, for the concentration distribution per particle size, the time-dependent data obtained from 45 channels of SMPS (5 nm – 1 μm) was used, whereas the particle size was categorized into ≤100 nm for nanoparticles and 100 nm – 1 μm for other particles. The count median diameter (CMD) and the mass median aerodynamic diameter (MMAD) were also presented for each condition. For the circulation time of nozzle extrusion, each cycle of the six extruder steppers was measured in triplicate and expressed as the arithmetic mean.

3. Results

3.1. Particle number and mass concentrations

Table 2 presents the results of measuring the particle number and mass concentrations according to the extruder temperature, nozzle extruding speed, and air flow rate. The SMPS device was used, the white ABS filament was provided as the material, the nozzle diameter was 0.4 mm, and the measurement interval was ~7 min. For each condition, the measurements were taken 11 times on average (8 – 13 times) for statistical analysis. As the extruder temperature increased from 210 ºC to 300 ºC, the circulation time was reduced, and the GM particle number and mass concentrations for particles ≤100 nm and particles of 100 nm – 1 μm increased. CMD and MMAD also showed an increasing tendency. The highest particle number was observed for particles ≤100 nm at nozzle extruding speed of level 5, and as the speed increased from level 5 to level 20, the circulation time was reduced. The GM particle number concentration for particles of 100 nm – 1 μm and the particle mass concentration for both ≤100 nm and 100 nm – 1 μm increased as the nozzle extruding speed increased, with an increase in CMD and MMAD. As the air flow rate increased from 20 LPM to 50 LPM, the GM particle number and mass concentrations for particles ≤100 nm increased, and the total GM of particle number concentration also increased. The

Table 2. Particle number concentration and mass concentration according to conditions

Condition	Value	Number concentration				Mass concentration				Extruder cycle time (sec)
		10~100 nm GM[a](GSD[b]) (#/m^3)	0.1~1 μm GM[a](GSD[b]) (#/m^3)	Total GM[a](GSD[b]) (#/m^3)	CMD[c] (nm)	10~100 nm GM[a](GSD[b]) (μg/m^3)	0.1~1 μm GM[a](GSD[b]) (μg/m^3)	Total GM[a](GSD[b]) (μg/m^3)	MMAD[d] (nm)	
Extruder temperature (°C)	210	1,538,351(1.10)	98,954(1.12)	1,635,450(1.09)	44.24	118.17(1.05)	91.70(1.17)	208.98(1.08)	87.35	151.17
	240	3.027,642(1.04)	568,347(1.03)	3,583,436(1.03)	56.38	333.55(1.03)	555.63(1.03)	860.73(1.02)	104.51	53.22
	270	4,340,624(1.02)	1,604,989(1.03)	5,886,919(1.01)	68.30	585.28(1.03)	1,814.87(1.03)	2309.48(1.02)	120.74	49.56
	300	4,980,785(1.04)	2,912,097(1.02)	7,765,549(1.03)	77.65	742.53(1.05)	4,029.42(1.02)	4615.88(1.02)	140.00	46.11
Extruding speed (level)	5	2,570,234(1.08)	262,545(1.09)	2,829,620(1.07)	48.57	232.70(1.05)	230.57(1.12)	454.99(1.04)	92.68	102.72
	10	2,535,466(1.01)	579,172(1.02)	3,096,274(1.01)	58.60	289.51(1.02)	585.28(1.03)	844.61(1.02)	109.23	51.61
	15	2,537,863(1.02)	782,594(1.04)	3,292,032(1.01)	64.26	317.42(1.02)	853.20(1.04)	1,127.22(1.03)	116.93	41.56
	20	2,485,600(1.01)	914,958(1.03)	3,364,020(1.01)	67.92	327.70(1.02)	1,036.82(1.04)	1,313.10(1.03)	121.23	36.61
Air flow rate (LPM)	20	2,043,253(1.07)	689,326(1.03)	2,710,453(1.05)	67.69	275.56(1.07)	729.70(1.04)	966.17(1.02)	115.86	60.56
	30	2,339,816(1.02)	600,831(1.03)	2,919,550(1.02)	60.31	273.88(1.02)	628.68(1.03)	870.22(1.02)	112.62	51.22
	40	2,734,589(1.02)	528,516(1.05)	3,246,321(1.01)	55.37	292.51(1.02)	520.56(1.06)	786.77(1.04)	105.98	50.22
	50	3,051,281(1.02)	422,939(1.04)	3,464,585(1.02)	51.70	302.12(1.02)	391.58(1.05)	675.50(1.03)	98.51	49.33

Analysis equipment: SMPS (measurement interval: 7 min; number of measurements; 11 times), Material: ABS filament (white color), Nozzle Diameter: 0.4 nm

[a]Geometric Mean, [b]Geometric Standard Deviation, [c]Count Median Diameter, [d]Mass Median Aerodynamic Diameter

GM particle number and mass concentrations for particles of 100 nm – 1 μm decreased, and the total GM of particle mass concentration also decreased with a tendency of decrease in CMD and MMAD. The extruder circulation time per air flow rate was the lowest (60.56 s) at 20 LPM, whereas the circulation time was similar; 51.22 s, 50.22 s, and 49.33 s, at the air flow rates of 30, 40, and 50 LPM, respectively.

3.2. Particle size distribution

Fig. 2 shows the particle size distribution according to extruder temperature, extruding speed, and air flow rate. With an increase in extruder temperature, an increasing tendency was found in the particle size for the GM particle number and the GM mass concentration, and the total particle number concentration and total mass concentration also increased (*Fig.* 2(a), (b)). As the nozzle extruding speed increased, the particle size for GM particle number and GM mass concentrations, which total particle number concentration and total mass concentration, also increased (*Fig.* 2(c), (d)). As the air flow rate increased from 20 LPM to 50 LPM, the particle size for the GM particle number concentration showed a decreasing tendency, whereas the total number concentration increased (*Fig.* 2(e)). In contrast, the GM particle mass concentration showed a decreasing tendency in particle size with increasing air flow rate, and the total mass concentration also decreased (*Fig.* 2(f)).

3.3. Particle size distribution and particle mass concentration

The weight of the aluminum foil filter connected to the ELPI per particle size was measured before and after collection, for 65 min from the time of stable generation and at 10 LPM air flow rate. The result of measuring the mass per particle size showed that approximately 80 % of the particles were of 60 nm-260 nm size, with 1.7 % particles of ≥1 μm size. The mass concentration using the Probit method[8] was 0.908 mg/m^3 (0.590 mg / (10 LPM × 65 min)), MMAD was 111 nm, and GSD was 2.10 (*Table* 3). In the graph of aerodynamic diameter and cumulative mass, the correlation coefficient was 0.98 and the gradient was 2.99, whereas the aerodynamic diameter of log normal distribution was mostly <0.5 μm, with a small distribution of 1 μm (*Fig.* 3).

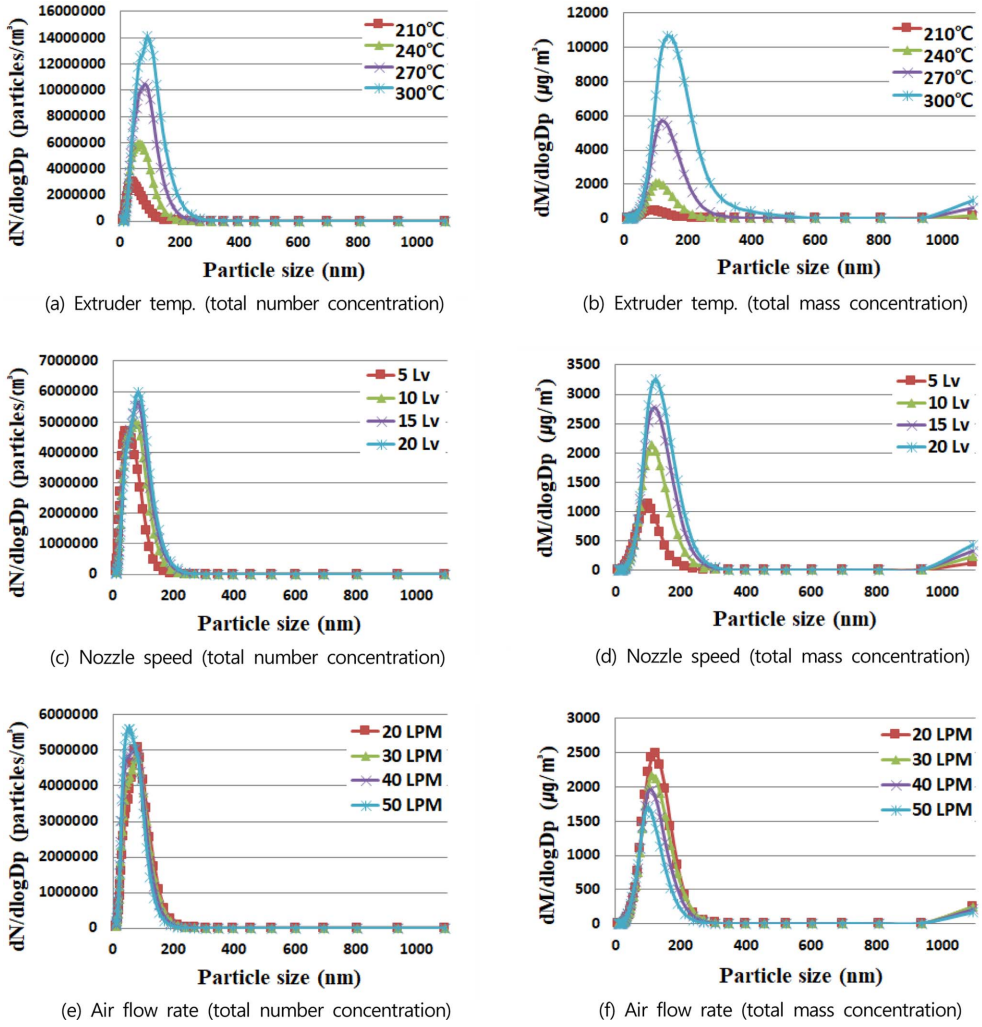

(a) Extruder temp. (total number concentration)

(b) Extruder temp. (total mass concentration)

(c) Nozzle speed (total number concentration)

(d) Nozzle speed (total mass concentration)

(e) Air flow rate (total number concentration)

(f) Air flow rate (total mass concentration)

Fig. 2. Particle size distribution according to nozzle extruder temperature, extruding speed, and air flow rate.

3.4. Stability

Fig. 4 shows the changes in particle number and mass concentrations as observed for 6 h under the recommended conditions of the 3D printer and filament manufacturers. The SMPS device was used and the white ABS filament was provided as the material. The extruder nozzle diameter was 0.4 mm, extruder temperature was 240 °C, air flow rate was 30 LPM, extruding speed was level 10, and the measurements were taken 90 times in the interval of ~4 min for statistical analysis. Increasing the extruder temperature caused the fusion of the filament, and the particle number and mass concentrations for ≤100 nm particles showed a steep increase. Stabilization began from approximately 30 min due to slowly decrease in concentration, and the stable levels were maintained until completion. The particle number and mass concentrations for particles >100 nm slowly increased from the onset of generation, and a stable level was maintained after approximately 30 min. From 30 min after the onset of generation until completion, the GM values of particle number concentration, mass concentration, and surface concentration were 2,929,026 #/cm^3, 775.15 μg/cm^3, and 44,829.86 μm^2/cm^3, respectively, and the GM particle size in each case was 56.69, 105.53, and 89.21 nm, respectively

Table 3. The ABS particle size distribution analysis by ELPI

Stage	Size range (μm)	Cut-off size (μm)	Initial Mass (mg)	Final Mass (mg)	Mass (mg)	Mass (%)	Cumulative Mass (%)
1	0.010 ~ 0.022	0.009919677	15.58	15.60	0.020	3.390	0.000
2	0.022 ~ 0.042	0.022218011	15.52	15.54	0.020	3.390	3.390
3	0.042 ~ 0.080	0.040539610	15.61	15.69	0.080	13.559	6.780
4	0.080 ~ 0.140	0.072020830	15.55	15.71	0.160	27.119	20.339
5	0.140 ~ 0.210	0.121346611	15.43	15.62	0.190	32.203	47.458
6	0.210 ~ 0.320	0.199587074	15.38	15.48	0.100	16.949	79.661
7	0.320 ~ 0.510	0.313737151	15.43	15.44	0.010	1.695	96.610
8	0.510 ~ 0.800	0.481367843	15.70	15.70	0.000	0.000	98.305
9	0.800 ~ 1.300	0.758122681	15.44	15.45	0.010	1.695	98.305
10	1.300 ~ 2.000	1.248198702	15.46	15.46	0.000	0.000	100.000
11	2.000 ~ 3.300	2.016730027	15.48	15.48	0.000	0.000	100.000
12	3.300 ~ 5.500	3.012772809	15.58	15.55	0.000	0.000	100.000
13	5.500 ~ 8.200	4.437431690	15.67	15.67	0.000	0.000	100.000
14	8.200 ~ 10.00	7.301766909	15.48	15.48	0.000	0.000	100.000
		10			0.590		100.000
					MMAD	0.111	
					GSD	2.10	

Analysis equipment: ELPI, Material: ABS filament (white color), Nozzle diameter: 0.4 mm, Nozzle temperature: 240 °C, Inlet air: 20 LPM, Nozzle number: 6 channel, Extruding stepper: 10 level, Sampling flow: 10 LPM, Sampling time: 65 minutes, Mass concentration: 0.908 mg/m^3, GSD: Geometric Standard Deviation

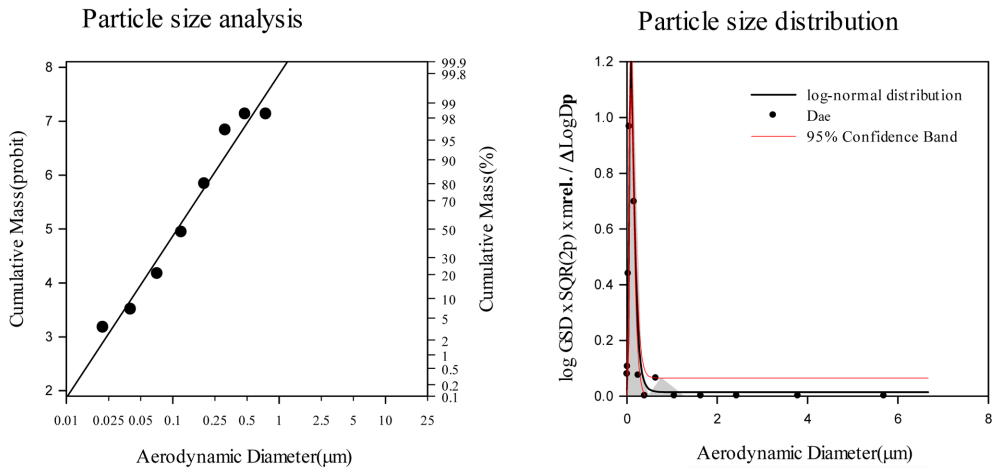

Fig. 3. Changes in particle number and mass concentration over time under manufacturer's recommended conditions.

(*Table* 4).

3.5. Particle morphology

The particles inside and outside the generation chamber were collected using the LC200-NI grid, and the particle morphology was observed using the TEM. The ABS particles were mostly of a circular shape and <10 nm in size, both inside and outside the generation chamber. As these circular particles underwent aggregation, a grape-shaped assembly of

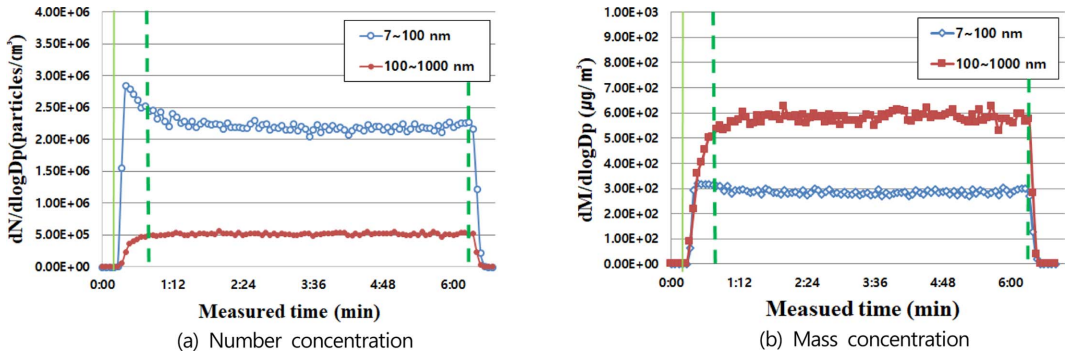

(a) Number concentration (b) Mass concentration

Fig. 4. Graph of the relationship between aerodynamic diameter and cumulative mass.

Table 4. Geometric average concentration and particle size under manufacturer's recommended conditions by SMPS

Item	Concentration GM[a](GSD[b]) (unit)	Particles concentration range (nm)	Particle size GM[a](GSD[b]) (nm)	Median size (nm)
Number Concentration	2,929,026(1.04) (1/cm^3)	2,717,558~3,425,397	56.69(1.68)	58.39
Mass Concentration	775.15(1.06) (μg/m^3)	504.73~829.27	105.53(1.48)	108.02
Surface Concentration	47,829.86(1.04) (μm^2/cm^3)	38,110.37~50,188.79	89.21(1.54)	92.67

Analysis equipment: SMPS (measurement interval: 4 min; number of measurements; 90 times), Material: ABS filament (white color), Nozzle diameter: 0.4 nm, Nozzle temperature: 240 °C, Inlet air: 30 LPM, Nozzle number: 6 channel, Extruding stepper: 10 level, Generator operating time: 6 hours

[a]Geometric Mean, [b]Geometric Standard Deviation

tens to hundreds of particles of nanometer size was formed (*Fig.* 5).

4. Discussion

Powder materials such as resin and epoxy resin lead to concurrent deposition of the adhesive due to the binder jetting upon production, which may cause the generation of a large quantity of organic compounds in addition to the nanometer-sized aerosol.[9] In contrast, the FDM involving the heating of a thermoplastic material causes the generation of far less quantity of HAPs. Although the 3D printing based on FDM led to the detection of organic compounds such as formaldehyde in addition to nanoparticles, the concentration was at a far lower level than the maximum exposure limit or at a level of background concentration that does not inflict harm on human health.[2,4,6,7,10] Thus, this study focused on the analysis of aerosol rather than HAPs.

The use of 3D printers outside the workplace has increased in frequency over time.[1,11-13] However, to conduct the printing in a poorly ventilated space for a prolonged time causes the generation of particulate and volatile substances that increase the health risk to the respiratory system and the eyes.[7] Stabile *et al.* [14] investigated various indoor conditions for 3D printing and reported that the range of mean aerosol release was 108~1,011 particles/min, and the concentration varied according to the printing speed and conditions, and the ABS filament was found to generate the largest quantity of aerosol. In addition, 3D printing in an office without any ventilation system was shown to substantially increase the generation of nanoparticles and their mass concentration, and the nanoparticles could still be detected 20 h after terminating the printing.[15] Recently, it has been confirmed that a science high school teacher who has used 3D printers a lot for classes has a successive rare cancer sarcoma. Without any exposure limit or regulation, the increased dispute on the safety of 3D printers has merely led the government and educational

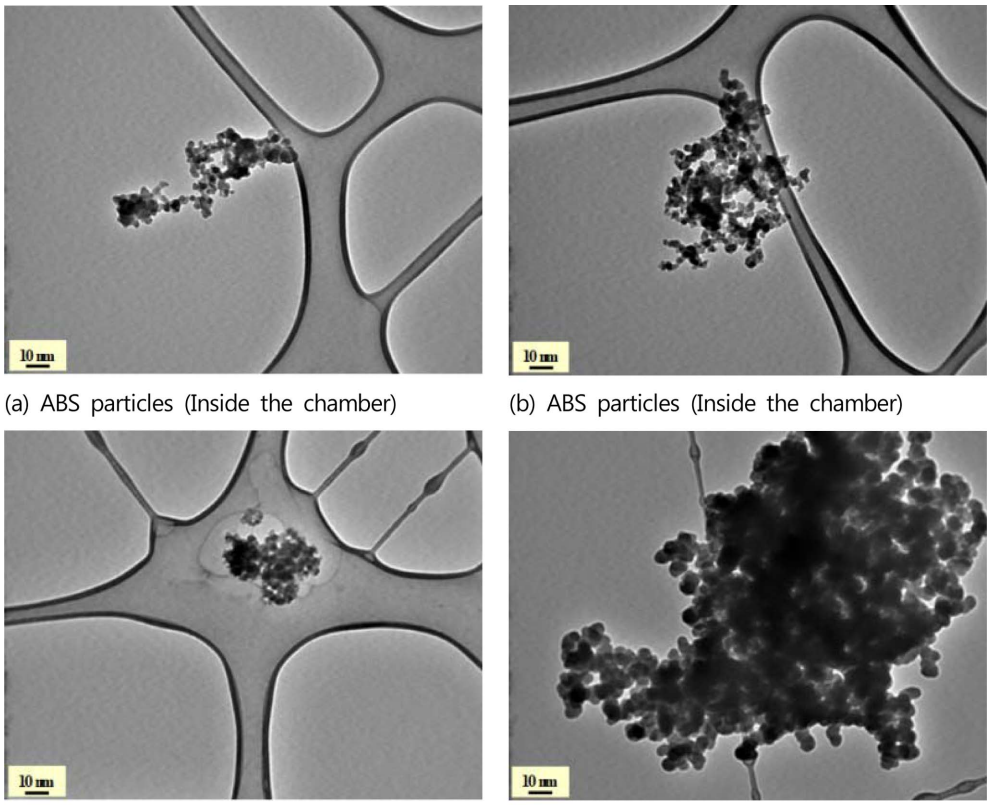

(a) ABS particles (Inside the chamber) (b) ABS particles (Inside the chamber)

(c) ABS particles (outside the chamber) (d) ABS particles (outside the chamber)

Fig. 5. TEM micrographs of ABS particles morphology (×50,000).

institutions to distribute a formal guidelines suggesting the restricted use of 3D printers, prohibit use in populated places, or restrict entrance to the place of 3D printing. However, the safety control measures have been seriously inadequate.[16,17] To establish a scientific basis for legal regulations including the safety control measures, a prerequisite would be to develop a nanoparticle generator through which biohazards could be assessed.

In the generation of nanoparticles according to the extruder temperature, the extruder circulation time was ≥ 3 times higher at 210 ºC compared to other temperature conditions, although it was set to level 10 in all conditions. The concentration of the generated particles was low, which may be attributed to the lower T_m (220-235 ºC) of ABS compared to the optimum nozzle temperature (225 ºC). At this temperature, the fusion of ABS filament is less active with consequent low level of particle generation. Nanoparticles are mostly caused by the heating process than the printing process, and as they are generated from the heat-deformation or decomposition of the filament during the time of heating inside the extruder, the extruder temperature is the key in nanoparticle generation.[3,5,14] This is considered to have caused the increase in both the particle number and mass concentrations of the particles of ≤100 nm and 0.1 – 1 μm as the temperature of the extruder was increased, with a simultaneous increase in CMD, MMAD, and the GM of the diameter. Furthermore, the GM of the particle number concentration at 300 ºC, which is higher than the manufacturer's recommended temperature of 240 ºC, was approximately 1.6 times higher for particles ≤100 nm and approximately 5.1 times higher for particles of 0.1 – 1 μm, whereas the GM of the particle mass concentration was approximately

2.2 times higher for particles ≤100 nm and approximately 7.2 times higher for particles of 0.1 – 1 μm.

For nozzle extruding speed, an increase in the extrusion level led to a fall in the circulation time of the extruder stepper, a circular transporting device for the nozzle, whereas the central diameter and the total GM of particle number and mass concentrations increased. Although the extruding speed was the sole influential factor, the circulation time of the extruder stepper increased by ≥ 2-fold at level 5 than in any other conditions, presumably due to the uncertainty from the mechanical limitation of the extruder controller. In general, an increase in the extruding speed reduces the particle number concentration, but in this study, the GM particle number concentration decreased for particles ≤100 nm. This may be attributed to the formation of particles ≥ 0.1 μm through the collision and aggregation of the particles escaping the generation chamber with a weakened state of electrostatic repulsion when the concentration of the nanoparticles increased above a certain level. The particle morphology on the interior and exterior of the chamber, as observed in the TEM analysis, showed that the particles existed as an aggregate assembly rather than independent nano-sized particles (*Fig.* 5).

The particles generated by the NMG were mostly circular in shape and <10 nm in size both inside and outside the generation chamber; however, the collision and condensation of these particles caused the formation of assemblies of tens to hundreds of nanometers in size. In a study by Deng *et al.*[3], an increase in the extruding speed led to an increase in the particle number concentration until the speed reached 60 mm/s, after which no further increase in the concentration was observed, which was considered to be due to the frequent aggregation of nanoparticles.

In the experiment based on the air flow rate, only the particles ≤100 nm showed higher GM values of the particle number concentration with an increase in the air flow rate, and all other measured values decreased. This is because the increased air flow led to a fall in the particle density for the particles ≤100 nm, which lowered the probability of particle collision and thus reduced the particle aggregation. Therefore, although the particle number concentration for particles of 0.1 – 1 μm decreased with increasing air flow, the particle number concentration for particles ≤100 nm and consequently the total particle number concentration increased, ultimately reducing the CMD or MMAD of the particles.

In the stability experiment, the particle number concentration, mass concentration, surface concentration, and particle size maintained stable without a notable deviation (*Fig.* 4, *Table* 4). The result is significant as the Inhalation Toxicity Test of the OECD Test Guidelines for Health Impact Assessment states that the exposure concentration should be maintained at a stable level with the mean concentration of the aerosol substance within ± 20 %[18,19] to verify the stability.

The SMPS device was used as it is relatively more efficient than the ELPI for prolonged monitoring. Nevertheless, the ELPI was concurrently used for the measurements regarding particles of 5 nm-1 μm size. The ELPI is based on the principle of collision in the collection of particles through an aluminum foil filter with an oil layer, and the particle bouncing upon the measurement of a high concentration for a long time (≥ 90 min on average) causes the particles to be expelled from the filter. Due to such phenomenon, the generated particles cannot be stably collected for a prolonged period, and the concentration decreases over time.[20] Thus, in this study, the ELPI was used for approximately 1 h to collect the particles and obtain the MMAD and GSD values. The result of the measurements showed that, although the particles ≥ 1 μm were not abundant, the relatively large mass of the particles in this interval influenced the mass concentration, leading to approximately 20 % higher values than those obtained from SMPS.

The NMG developed in this study was shown to have the following benefits: i) the particle size and concentration can be adjusted based on the extruder temperature, nozzle extruding speed, and air flow rate; ii) these conditions can be easily manipulated via the controller; and iii) the nanoparticles can be continuously generated in an identical concentration. In this study, the

aerosol particles containing nanoparticles could be generated and transferred at a stable level and constant concentrations for a long time, to verify the potential use of the novel generator in the impact assessment of nanoparticle biotoxicity. An additional study should be conducted regarding the reproducibility and the dose-response evaluation through *in vivo* tests under the same conditions. The findings will allow the impact assessment of nanoparticles related to the living body.

5. Conclusions

This study developed a novel NMG that can be used in the impact assessment of nanoparticle biotoxicity. As the extruder temperature increased, the GM particle number and mass concentrations, CMD and MMAD increased for both ≤100 nm and 100 nm – 1 μm particles. As the nozzle extruding speed increased, the total GM values of the particle number and mass concentrations increased, with higher CMD and MMAD. However, for particles ≤100 nm, the generated number of particles decreased with increasing nozzle extruding speed. As the flow rate of the supplied air increased, the GM particle number and mass concentrations of particles ≤100 nm and the total GM values of the particle number concentration increased. The increased air flow rate also reduced the GM particle number and mass concentrations of 100 nm – 1 μm particles and the total GM particle number concentration, as well as CMD and MMAD. In the generation for 6 h, the concentration was maintained at a stable level from the onset of generation to 30 min after the completion. The particle distribution analyzed using the ELPI showed that 60 nm – 260 nm particles accounted for approximately 80 % and particles ≥ 1 μm accounted for 1.7 %. The mass concentration was 0.908 mg/m^3 with 111 nm MMAD and 2.10 GSD. The ABS particles on the interior and exterior of the chamber were mostly <10 nm and in a circular shape, and such circular particles aggregate to form a grape-shaped assembly of tens to hundreds of nanometers in size.

The novel NMG developed in this study showed a pattern of constant particle number and mass concentrations and particle size according to the extruder temperature, nozzle extruding speed, and air flow rate. The findings indicated that the particle concentration could be maintained at a stable level through the real time adjustment of conditions such as particle size and concentrations and the stability was prolonged. Thus, the novel NMG can be used in the assessment of the impact of nanoparticles on the living body, which will provide a scientific basis for establishing exposure standards and legal regulations in the working environment for the evaluated substance, and ultimately preventive health hazards on workers.

Acknowledgements

This study was conducted as part of the Chemical Substances Research Project of the Occupational Safety and Health Research Institute, Ministry of Employment and Labor.

References

1. B. Stephens, P. Azimi, E. O. Zeineb and R. Tiffanie, *Atmospheric Environment*, **79**, 334-339 (2013).
2. Y. Kim, C. Yoon, S. Ham, J. Park, S. Kim, O. Kwon and P. J. Tsai, *Environ. Sci. Technol.*, **49**(20), 12044-12053 (2015).
3. Y. Deng, S. J. Cao, A. Chen and Y. Guo, *Building and Environment*, **104**, 311-319 (2016).
4. P. Azimi, D. Zhao, C. Pouzet, N. E. Crain and B. Stephens, *Environ. Sci. Technol.*, **50**(3), 1260-1268 (2016).
5. J. H. Park, H. J. Jeon, K. H. Park and C. S. Yoon, *J. Environ. Health Sci.*, **44**(6), 524-538 (2018).
6. E. L. Floyd, J. Wang and J. L. Regens, *J. Occup. Environ. Hyg.*, **14**(7), 523-533 (2017).
7. The Danish Environmental Protection Agency, 'Risk assessment of 3D printers and 3D printed products', Environmental Protection Agency, 2017.
8. J. M. Suh, W. Bin, S. H. Jang, J. H. Park and J. C. Choi, *Journal of Korean Society of Occupational and Environmental Hygiene*, **24**(4), 453-461 (2014).
9. N. Afshar-Mohajer, C. Y. Wu, T. Ladun, D. A. Rajon and Y. Huang, *Building and Environment*, **93**(2), 293-

301 (2015).
10. A. B. Stefaniak, A. R. Johnson, S. du Preez, D. R. Hammond, J. R. Wells, J. E. Ham, R. F. LeBouf, K. W. Menchaca, S. B. Martin, M. G. Duling, L. N. Bowers, A. K. Knepp, F. C. Su, D. J. de Beer and J. L. du Plessis, *Journal of Chemical Health and Safety*, **26**, 19-30 (2019).
11. Y. Zhou, X. Kong, A. Chen and S. Cao, *Procedia Engineering*, **121**, 506-512 (2015).
12. A. B. Stefaniak, R. F. LeBouf, M. G. Duling, J. Yi, A. B. Abukabda, C. R. McBride and T. R. Nurkiewicz, *Toxicol. Appl. Pharmacol.*, **335**, 1-5 (2017).
13. I. Gümperlein, E. Fischer, G. Dietrich-Gümperlein, S. Karrasch, D. Nowak, R. A. Jörres and R. Schierl, *Indoor Air*, **28**(4), 611-623 (2018).
14. L. Stabile, M. Scungio, G. Buonanno, F. Arpino and G. Ficco, *Indoor Air*, **27**, 398-408 (2017).
15. P. Steinle, *Journal of Occupational and Environmental Hygiene*, **13**, 121-132 (2016).
16. http://www.ohmynews.com/NWS_Web/View/at_pg.aspx?CNTN_CD=A0002663757&CMPT_CD=P0010&utm_source=naver&utm_medium=newsearch&utm_campaign=naver_news, Assessed 3 August 2020.
17. http://www.ohmynews.com/NWS_Web/View/at_pg.aspx?CNTN_CD=A0002670018&CMPT_CD=P0010&utm_source=naver&utm_medium=newsearch&utm_campaign=naver_news, Assessed 25 August 2020.
18. OECD Guidelines on the testing of chemicals Section 4 Health Effects Test No. 412 (25 June 2018), OECD.
19. OECD Guidelines on the testing of chemicals Section 4 Health Effects Test No. 413 (25 June 2018), OECD.
20. Dekati. In 'ELPI+ User manual', Ver.1.12 p.60, Dekati Ltd.; 2011.

Authors' Positions

Sung-Bae Lee : Senior Researcher
Jeong-Hee Han : Senior Researcher
Tae-Hyun Kim : Manager
Hyo-Keun Cha : Manager
Cheal-Hong Lim : Chief Researcher